Trajectory Optimization for Shared Control of Lower-Extremity Assistive Exoskeletons

Taylor M. Higgins, Gabriel Bravo-Palacios, James P. Schmiedeler, and Patrick M. Wensing

I. INTRODUCTION

Optimization-based control is a common approach for controlling many robotic systems, including legged robots [1], [2]. Some work has been done to use optimization strategies for exoskeleton control [3], for instance, to re-shape the reference trajectory for an upper-limb exoskeleton that used an impedance control method [4]. This abstract presents a nonlinear programming-based optimization strategy that solves simultaneously for the constrained exoskeleton state and control trajectories that incorporate the user's torque inputs and gait intentions in a safe manner. To do so, the user's torque inputs and desired gait features (e.g., desired gait speed [5]) must be estimated in advance. There are many strategies for intent recognition [5], [6] and time-series forecasting that could accomplish this task, including neural network modeling, Gaussian process regression, and others [7], [8]. These models can be trained by collecting torque measurements at each exoskeleton joint or, in the absence of torque sensors, based on disturbance observation [4]. This abstract establishes a trajectory optimization solution for a robotic exoskeleton that incorporates the user's torque inputs and gait intentions, assumed to be estimated a priori. The contribution is a proof of concept for using trajectory optimization to solve for the robot actions that realize the human's desired gait speed, to coordinate with predicted human torque input, and to assist wherever necessary such that the system progresses safely through the normal phases of gait.

II. METHODS

The exoskeleton model used for trajectory optimization is based on the EksoGT by Ekso Bionics, which has two legs, each with a powered hip and knee joint. Since the EksoGT is a proprietary device, the exact inertial properties of each segment have not been published. This work models the exoskeleton as a five-link planar device with each segment idealized as a thin rod. The overall mass of the exoskeleton is 20.41 kg, and the lengths of each segment are adjustable such that they match the human user. The total mass was divided among the segments such that the trunk segment had 66.66% of the total mass, while each thigh and shank had 10% and 6.67%, respectively. The optimization was run with and without additional human/exoskeleton forces and torque applied at the end of the lower leg segment, to represent the addition or lack of a powered ankle joint.

Joint torque and joint angle trajectories were extracted for one gait cycle of one subject walking at 1.2 m/s from [9]. The leg length for this subject was gleaned from the average height of the right greater trochanter marker (1.06m). Based on proportions in [10], this leg length corresponds with a thigh length of 0.39 m and a lower leg length (including the foot) of 0.53 m. The total mass of the subject was assumed to be 66.1 kg, based on a colleague's weight who had a similar leg length. The center of mass (COM), mass, and moment of inertia for each segment of the human body were then calculated following the anthropometric relationships reported in [10]. Finally, the human was assumed to be rigidly attached to each exoskeleton segment with shared degrees of freedom (DOFs) perfectly aligned such that combined inertial parameters were calculated by adding masses, calculating the new COM, and using the parallel axis theorem to combine moments of inertia about the new COM. For the combined human/exoskeleton model, the torso segment represents the combined head, arms, and trunk.

Given these parameters of the human/exoskeleton model, the general form of the optimal control problem is

$$\min_{\mathbf{x}(\cdot),\mathbf{u}(\cdot),\mathbf{p}(\cdot)} \quad V(t_0,t_f,\mathbf{x}(\cdot),\mathbf{u}(\cdot),\mathbf{p}(t)), \tag{1}$$

$$\text{subject to} \quad \dot{\mathbf{x}} = \mathbf{f}(t,\mathbf{x}(t),\mathbf{u}(t),\mathbf{p}(t)), \tag{2}$$

$$\mathbf{h}(t,\mathbf{x}(t),\mathbf{u}(t),\mathbf{p}(t)) \leq 0, \tag{3}$$

$$\mathbf{g}(t_0,t_f,\mathbf{x}(t_0),\mathbf{x}(t_f),\mathbf{p}(t)) \leq 0, \tag{4}$$

where decision variables include the state and exoskeleton control trajectories, $\mathbf{x}(t) \in \mathbb{R}^7$ and $\mathbf{u}(t) \in \mathbb{R}^4$, initial and final times, t_0 and t_f, and optimization variables $\mathbf{p}(t)$ that include ground reaction forces and foot locations. Equation 1 includes the cost function, $V(\cdot)$, while Eqs. 2, 3, and 4 represent the dynamics, path, and boundary constraints. The human torque contributions are added as external torques in the dynamics equation.

The cost function was configured to contain four terms,

$$\begin{aligned} V(\cdot) =& w_p\|\mathbf{t}_\mathrm{E} - \mathbf{t}_\mathrm{H}\|^2 + w_v\|v_\mathrm{H} - v_\mathrm{E}\|^2 + \ldots \\ & \int_0^{T_{tot}} \left[w_t\|\mathbf{u}(t)\|^2 + w_q\|\mathbf{q}_H(t) - \mathbf{q}_E(t)\|^2\right] dt, \end{aligned} \tag{5}$$

where the first term penalizes the difference in the amount of time spent within each gait phase between the human data and the optimized exoskeleton trajectory, organized by vectors $\mathbf{t}_\mathrm{H}$ and $\mathbf{t}_\mathrm{E}$, respectively. The second term penalizes the difference between the human's desired average forward

This work was supported in part by the National Science Foundation, under Grant IIS-1734532.

All authors are from the Department of Aerospace and Mechanical Engineering at the University of Notre Dame tgambon@nd.edu

speed (1.2 m/s in this case) and the optimized exoskeleton average forward speed, v_{H} and v_{E}, respectively. Next, the control torques $\mathbf{u}(t)$ and the difference between the human and exoskeleton joint angle trajectories, $\mathbf{q}_H(t)$ and $\mathbf{q}_E(t)$, are penalized at every time step.

Weights w_p, w_v, and w_q were set at 10^6, 10^6, and 10^3, respectively, while w_t was 10^{-5}, effectively prioritizing matching the human trajectory despite increased exoskeleton torques. The joint states were constrained for the safety of the human as follows: $-5^\circ \leq \theta \leq 15^\circ$ (to avoid overextending the back, or non-normative trunk lean), $-45^\circ \leq q_{t1,2} \leq 35^\circ$ (roughly the same range as the human data), $-1^\circ \leq q_{s1,2} \leq 80^\circ$ (to avoid hyperextending the knee), where clockwise is positive. The joint torques were constrained to be less than or equal to 300 Nm in magnitude to find solutions that are reasonable for existing motor technology. The optimization problem was solved for no human torque contribution, half human torque contribution, and full human torque contribution for both the ankle and no-ankle configuration.

The NLP problem was formulated in MATLAB with the aid of CasADi, an open-source tool for nonlinear optimization and algorithmic differentiation [11]. CasADi employs IPOPT, an Interior Point OPTimizer [12]. For this work, the third-party HSL solver ma97 was used [13].

III. Results and Discussion

IPOPT was able to solve for the exoskeleton trajectories that best incorporated the human torque inputs while also getting as close as possible to the user's intended gait speed, phase timing, and joint trajectories. The results for including/excluding ankle contributions are shown in Fig. 1. For the no-ankle condition, across all four joint angle trajectories for the full human torque condition, the root mean squared error (RMSE) was 7.77°, with a maximum error of 31°.

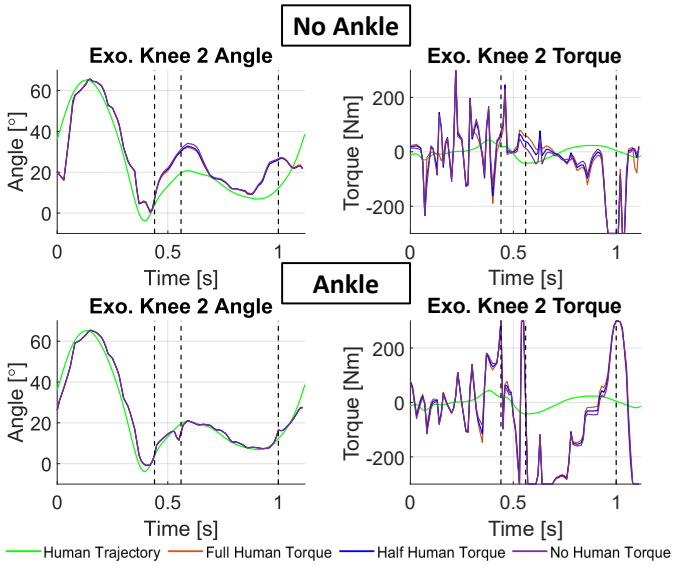

Fig. 1. Optimal knee angle and torque trajectories for various torque contributions by the human with $w_t = 10^{-5}$ and both the no-ankle and ankle configurations. Vertical dashed black lines demarcate the gait phases.

With the addition of ankle torque contributions, the solution was better able to match the human joint trajectories. Across all four joints, the RMSE was 3.70°, with a maximum error of 13°. Since the optimization barely penalized exoskeleton torques, the solution used large torques that often reached the maximum of 300 Nm to better match the human joint trajectories. The solution changed negligibly in response to changing human torques. By increasing w_t, the solutions can be coerced to forego matching the human trajectories in favor of reducing torque. While one might expect that increasing the human torque contribution with a higher value of w_t would result in lower overall exoskeleton torque, this was only the case for some sections of the gait cycle.

IV. Conclusions

Trajectory optimization has proven to be a highly flexible method for determining the appropriate exoskeleton control actions that incorporate human inputs and safety constraints. Although the current EksoGT does not have them, the results show that the addition of powered ankles allow the human/exoskeleton system to better track normative human joint trajectories, which is an important aspect of gait therapy. Furthermore, the weights in the cost function provide a way to easily shift the priorities of the optimization among several possible rehabilitation-relevant goals.

References

[1] R. Budhiraja, J. Carpentier, *et al.*, "Differential Dynamic Programming for Multi-Phase Rigid Contact Dynamics," *IEEE-RAS International Conference on Humanoid Robots*, pp. 53–58, 2019.

[2] J. Carlo, P. Wensing, *et al.*, "Dynamic Locomotion in the MIT Cheetah 3 Through Convex Model-Predictive Control," *MIT Open Access*, 2018.

[3] R. Huang, H. Cheng, *et al.*, "Optimisation of Reference Gait Trajectory of a Lower Limb Exoskeleton," *International Journal of Social Robotics*, vol. 8, no. 2, pp. 223–235, 2016.

[4] X. Wu, Z. Li, *et al.*, "Reference Trajectory Reshaping Optimization and Control of Robotic Exoskeletons for Human-Robot Co-Manipulation," *IEEE Transactions on Cybernetics*, vol. 50, no. 8, pp. 3740–3751, 2020.

[5] T. Gambon, J. Schmiedeler, *et al.*, "User Intent Identification in a Lower-Extremity Exoskeleton via the Mahalanobis Distance," *IEEE RAS/EMBS International Conference on Biomedical Robotics & Biomechatronics*, pp. 1115–1121, 2020.

[6] ——, "Effects of User Intent Changes on Onboard Sensor Measurements during Exoskeleton-Assisted Walking," *IEEE Access*, vol. 8, pp. 224 071–224 082, 2020.

[7] B. Fang, Q. Zhou, *et al.*, "Gait Neural Network for Human-Exoskeleton Interaction," *Frontiers in Neurorobotics*, vol. 14, no. October, pp. 1–10, 2020.

[8] M. Narayan and A. Fey, "Developing a novel force forecasting technique for early prediction of critical events in robotics," *PLoS ONE*, vol. 15, no. 5, pp. 1–34, 2020.

[9] E. Reznick, K. R. Embry, *et al.*, "Lower-limb kinematics and kinetics during continuously varying human locomotion," *Scientific Data*, vol. 8, no. 1, pp. 1–12, 2021.

[10] D. Winter, *Biomechanics and Motor Control of Human Movement*, 4th ed. Hoboken, New Jersey: John Wiley & Sons, 2009.

[11] J. Andersson, J. Gillis, *et al.*, "CasADi: a software framework for nonlinear optimization and optimal control," *Math Program*, vol. 11, no. 1, 2019.

[12] A. Wächter and Lorenz T. Biegler, "On the implementation of an interior-point filter line-search algorithm for large-scale nonlinear programming," *Mathematical Programming*, vol. 106, no. 1, pp. 25–57, 2006.

[13] STFC Rutherford Appleton Laboratory, "The HSL Mathematical Software Library." [Online]. Available: https://www.hsl.rl.ac.uk/